

Diffusive anomalies in a long-range Hamiltonian system

Luis G. Moyano

Centro Brasileiro de Pesquisas Físicas–Rua Xavier Sigaud 150, 22290-180, Rio de Janeiro, Brazil

Celia Anteneodo

Departamento de Física, Pontifícia Universidade Católica do Rio de Janeiro, CP 38071, 22452-970 Rio de Janeiro, Brazil

(Received 23 January 2006; published 17 August 2006)

We scrutinize the anomalies in diffusion observed in an extended long-range system of classical rotors, the HMF model. Under suitable preparation, the system falls into long-lived quasi-stationary states for which superdiffusion of rotor phases has been reported. In the present work, we investigate diffusive motion by monitoring the evolution of full distributions of unfolded phases. After a transient, numerical histograms can be fitted by the q -Gaussian form $P(x) \propto \{1 + (q-1)[x/\beta]^2\}^{1/(1-q)}$, with parameter q increasing with time before reaching a steady value $q \approx 3/2$ (squared Lorentzian). From the analysis of the second moment of numerical distributions, we also discuss the relaxation to equilibrium and show that diffusive motion in quasistationary trajectories depends strongly on system size.

DOI: 10.1103/PhysRevE.74.021118

PACS number(s): 05.90.+m, 05.20.-y, 05.60.Cd

I. INTRODUCTION

Systems with long-range interactions constitute a very appealing subject of research as they display a variety of dynamic and thermodynamic features very different from those of short-range systems treated in the textbooks (see [1] for a review on the subject). Moreover, in recent years, the study of long-range models has raised a renewed interest due to the presumed applicability of “nonextensive statistics” [2] to such systems.

A very simple model that offers the possibility of investigating many issues related to long-range interactions is the Hamiltonian mean-field (HMF) model [3]. It consists of N planar classical spins interacting through infinite-range couplings. The dynamical variables of each spin i are a phase angle θ_i and its conjugate momentum p_i whose evolution derives from the Hamiltonian

$$H = \frac{1}{2} \sum_{i=1}^N p_i^2 + \frac{1}{2N} \sum_{i,j=1}^N [1 - \cos(\theta_i - \theta_j)]. \quad (1)$$

This model can be seen as a variant of the XY ferromagnet, equipped with a natural Newtonian dynamics. Although the range of interactions is infinite, the HMF has been shown to behave in many aspects qualitatively like its long (finite)-range analogs [4]. Then, despite its simplicity, it reflects features of real systems with long-range forces such as galaxies and charged plasmas [1].

Its equilibrium thermodynamics can be solved in the canonical ensemble. It presents a ferromagnetic second-order phase transition, from a low-energy clustered phase to a high-energy homogeneous one that occurs at critical temperature $T_c=0.5$ (i.e., critical specific energy $\varepsilon_c=0.75$) [3]. However, concerning the microscopic dynamics, the system may get trapped into trajectories over which averaged quantities remain approximately constant during long periods of time with values different from those expected at equilibrium. For instance, for *water-bag* initial conditions (i.e., $\theta_i = 0 \forall i$, and p_i randomly taken from a uniform distribution), a quasistationary (QS) state appears at energies close to be-

low ε_c [5]. In a QS state, the nonequilibrium temperature (twice the specific mean kinetic energy) is almost constant in time and lower than the canonical value to which it eventually relaxes. However, the duration of QS states increases with the system size N , indicating that these states are indeed relevant in the ($N \rightarrow \infty$) thermodynamical limit (TL).

Several other peculiar features have been reported for out-of-equilibrium initial conditions, e.g., negative *dynamically effective* specific heat [3], non-Maxwellian momentum distributions [5–7], glassy dynamics [8], aging [9,10], anomalous diffusion [11,12], and others. In particular, anomalous diffusion has been initially associated to quasistationarity [11,12] and later to the (nonstationary) relaxation to equilibrium [13]. Moreover, controversies about the characterization of these states have arisen [10,14,15]; some aspects of the anomaly in diffusion have yet to be investigated. In this work, we present results on anomalous diffusion and relaxation to equilibrium, focusing on the dependence on system size.

II. RESULTS

The equations of motion derived from Eq. (1),

$$\begin{aligned} \dot{\theta}_i &= p_i \quad \text{for } 1 \leq i \leq N, \\ \dot{p}_i &= M_y \cos \theta_i - M_x \sin \theta_i, \end{aligned} \quad (2)$$

where $\vec{M} = \frac{1}{N} \sum_j (\cos \theta_j, \sin \theta_j)$ is the magnetization, were solved by means of a symplectic fourth-order algorithm [16]. Integrations were performed for fixed $\varepsilon=0.69$, for which quasistationary effects are more pronounced. Moreover, in the continuum limit, QS trajectories at energies around that value are stable stationary solutions of the Vlasov equation [6,7]. We considered two classes of initial conditions. One of them, which we will call “fully magnetized,” is a slight variation of *water-bag* initial conditions normally used in the literature: setting $\theta_i=0$ for $i=1, \dots, N$, and regularly valued momenta with the addition of a small noise (instead of ran-

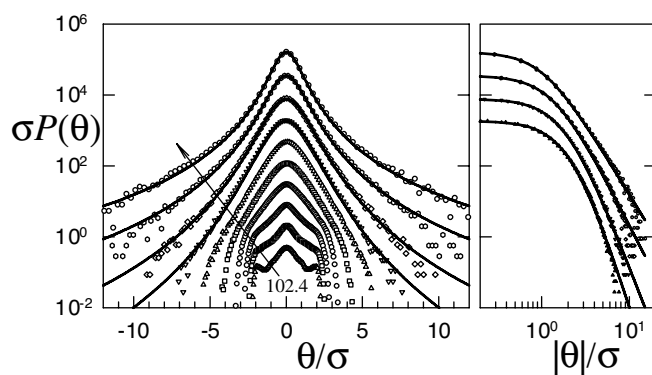


FIG. 1. Histograms of rotor phases at different instants of the dynamics (symbols). Simulations for $N=1000$ were performed starting from fully magnetized initial conditions at $\varepsilon=0.69$ (conditions leading to QS states). Countings were accumulated over 1000 realizations, at times $t_k=102.4 \times 2^k$, with $k=1, 2, \dots, 9$, growing in the direction of the arrow up to $t=52\,428.8$. Solid lines correspond to q -Gaussian fittings. Histograms were shifted for visualization. Right-side panel: log-log representation of the fitted data.

dom uniformly distributed ones). Under this preparation, the system gets trapped into paradigmatic QS states that present the main qualitative features of those formed by starting from random water-bag initial conditions [6,17], but the QS temperature T_{QS} is even lower and the duration of the QS regime is longer, in some way mimicking larger systems with a lower computational cost. We also performed simulations for equilibrium (EQ) initial conditions, waiting an appropriate transient after picking spatial coordinates and momenta from Boltzmann-Gibbs statistics.

Integration of Eqs. (2) yields phases in $(-\infty, \infty)$. Then, we built the histograms of phases at different times, accumulating the data over several realizations to improve the statistics. Actually, the dynamics depends on the phases modulo 2π , since they enter into the equations of motion as argument of sine and cosine functions. However, the statistics of unbounded phases is relevant as it reflects features of momentum space, which displays anomalies such as non-Maxwellian distributions [5] and two-time correlations signaling “aging” effects [10].

For low energies, phases are confined, while for sufficiently large energies, they evolve in diffusive motion [11]. In Fig. 1, we show the scaled histograms of rotor phases at different times, for fixed size ($N=1000$) and energy per particle $\varepsilon=0.69$, starting from fully magnetized initial conditions. After transient stages, histogram profiles can be described in good approximation, over the whole range, by the q -Gaussian function [2]

$$P(\theta) = A[1 + (q-1)(\theta/\beta)^2]^{1/(1-q)}, \quad (3)$$

where A is a normalization factor and β a positive constant. This function includes the standard Gaussian when $q \rightarrow 1$ and presents power-law tails for $q > 1$. Recalling that the probability density function (PDF) given by Eq. (3) has variance $\sigma^2 = \beta^2/(5-3q)$, for $q < 5/3$, and considering normalized angles $\phi = \theta/\sigma$, then Eq. (3) can be written as the uniparametric function

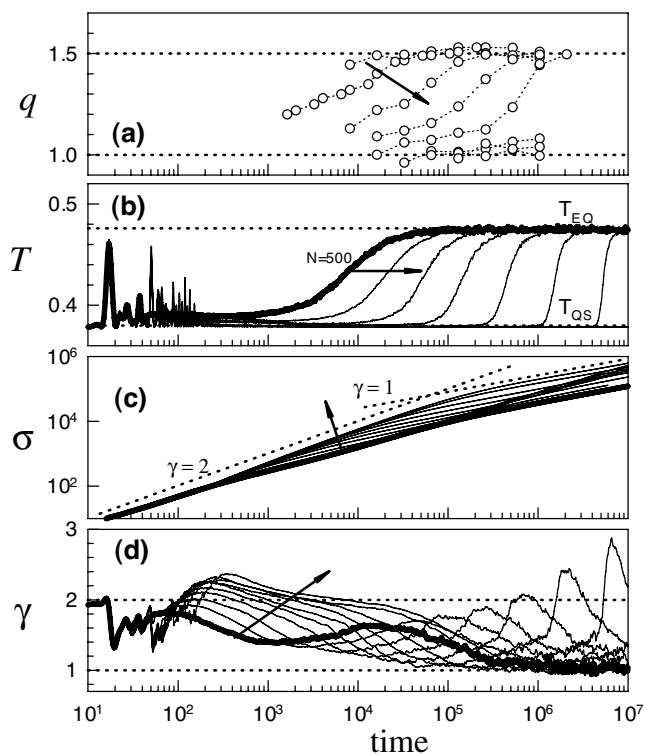


FIG. 2. Averaged time series of (a) parameter q (symbols), (b) temperature T , (c) deviation σ , and (d) diffusion exponent γ , for $\varepsilon=0.69$ and different values of N ($N=500 \times 2^k$, with $k=0, \dots, 9$). Bold lines correspond to $N=500$, as reference, and N increases in the direction of the arrows up to $N=256\,000$. Averages were taken over $2.56 \times 10^5/N$ realizations, starting from a *fully magnetized* configuration at $t=0$. Although small numbers of realizations are used for large sizes, curves are reproducible. In panel (a), the fitting error is approximately 0.03. Dotted lines are drawn as reference. In (b), they correspond to temperatures at equilibrium ($T_{EQ}=0.476$) and at QS states in the TL ($T_{QS}=0.38$). In (c), they correspond to ballistic motion ($\gamma=2$) and to normal diffusion ($\gamma=1$).

$$P_q(\phi) = A_q \left(1 + \frac{q-1}{5-3q} \phi^2 \right)^{1/(1-q)}, \quad (4)$$

with $A_q = \sqrt{\frac{q-1}{\pi(5-3q)}} \frac{\Gamma(1/(q-1))}{\Gamma(1/(q-1)-1/2)}$. At each instant t of the dynamics, σ^2 is computed as

$$\sigma^2(t) = \langle (\theta - \langle \theta \rangle_t)^2 \rangle_t, \quad (5)$$

where $\langle \dots \rangle_t$ denotes the average over the N rotors and over different realizations of the dynamics at time t . Although q -Gaussian PDFs naturally arise within nonextensive statistics, we cannot establish a straightforward link in the present context. Anyway, this simple fitting expression allows a phenomenological characterization of the shape of numerical histograms as a whole. In this sense, the single parameter q contains more information than, for instance, the second moment of the distribution. Hence, one can follow histogram evolution and, in particular, detect its possible convergence to some attractor shape.

In Fig. 2(a), the evolution of q for different sizes N is

displayed. Notice in Fig. 1 that at short times the histograms are not strictly Gaussian, however they can be progressively approximated by q -Gaussians with parameter q increasing up to a steady value, which for all N falls within the range $q \approx 1.51 \pm 0.02$. In Fig. 2, we also show the temporal evolution of the nonequilibrium temperature $T(t) = \sum_i \langle p_i^2 \rangle / N$ [Fig. 2(b)] and dispersion $\sigma(t)$ [Fig. 2(c)]. Although similar plots have already been reported elsewhere for QS states, Figs. 2(b) and 2(c) were included in order to exhibit the parallel among the different stages of the relevant quantities. Instead of single runs, averaged quantities are presented. Since they are much less noisy, they allow the representation of several curves in the same plot without distorting the mean features observed in individual runs. We can see that q attains a steady value approximately when the QS \rightarrow EQ transition is completed.

Diffusion of spatial coordinates can be described through the temporal behavior of the average squared displacement $\sigma^2(t)$ as defined by Eq. (5). In the one-dimensional generalized Einstein relation

$$\sigma^2(t) = 2Dt^\gamma, \quad (6)$$

where D is a constant, the case $\gamma=1$ corresponds to normal diffusion, $\gamma < 1$ to sub-diffusion, and superdiffusion occurs for $\gamma > 1$. In order to detect different regimes, it is useful to obtain an instantaneous exponent γ as a function of time by taking the logarithm in both sides of Eq. (6) and differentiating with respect to $\ln t$,

$$\gamma(t) = \frac{d(\ln \sigma^2)}{d(\ln t)}. \quad (7)$$

The outcome of this procedure can be seen in Fig. 2(d).

In Fig. 3, the same information contained in Fig. 2 is presented for rescaled times. The chosen scaling ($t/N^{1.7}$) allows approximate collapse of the inflection points in the temperature plot. This scaling has already been considered in the literature before, although for different preparations also leading to QS states (water-bag [14] and zero magnetization [13] initial conditions). An intermediate scale between N and N^2 is in fact expected theoretically for relaxational features [18].

The histograms of rotor phases, for $N=500$ and $\varepsilon=0.69$, but starting from an equilibrium configuration, are shown in Fig. 4. In this case, histogram shapes present pronounced shoulders that persist for long times and cannot be well described by q -Gaussian functions. However, as times goes by, the shoulders shift away from the center and the histograms tend to a q -Gaussian function, with q going to $q \approx 3/2$ from above in the long-time limit. The corresponding evolution of σ and γ is shown in Fig. 5.

Then, both starting from equilibrium and from out-of-equilibrium (fully magnetized) configurations, initially confined distributions of phases develop long tails and adopt a q -Gaussian form (squared Lorentzian). Of course, in all cases, the distributions of angles folded onto the interval $(-\pi, \pi]$, through an appropriate modulo 2π operation, present the shapes already known (see [19]), either for equilibrium or for out-of-equilibrium situations.

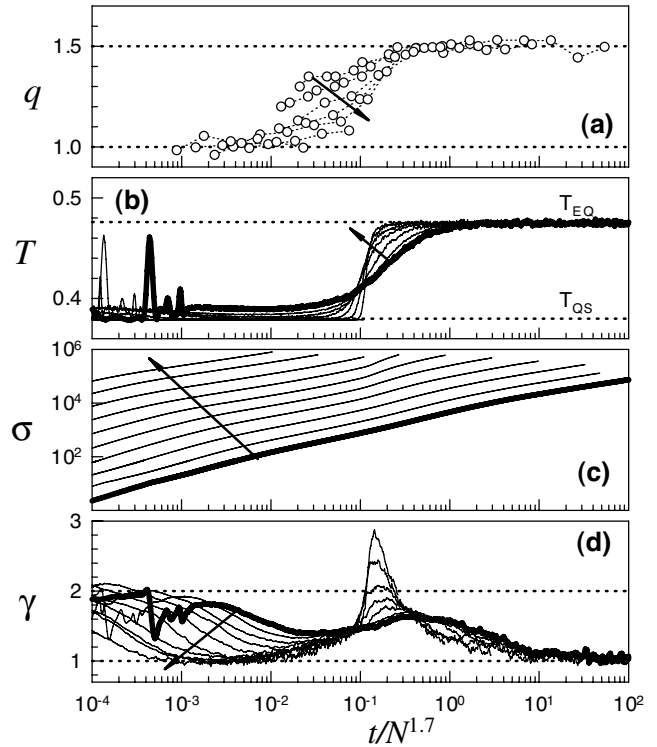


FIG. 3. Averaged time series of (a) parameter q (symbols), (b) temperature T , (c) deviation σ , and (d) local exponent γ , as a function of $t/N^{1.7}$. Data are the same as presented in Fig. 2.

For the latter class of initial conditions, phase motion is ballistic ($\gamma=2$) at short time scales in which rotors move almost freely, while phases display normal diffusion ($\gamma=1$) in the long-time limit, as shown in Fig. 5 (see also [13]). The crossover time between both behaviors shifts to larger times as N increases, growing linearly with N . A similar pattern of behaviors is also observed at supercritical energies ($\varepsilon=5$).

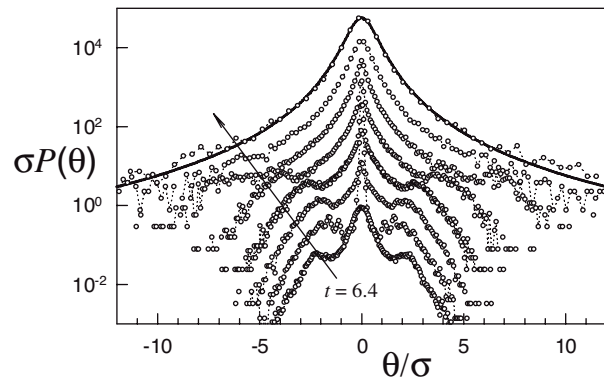


FIG. 4. Histograms of rotor phases at different instants of the dynamics (symbols). Simulations were performed for $N=500$ and $\varepsilon=0.69$, starting from an equilibrated initial condition. Countings were accumulated over 200 realizations, at times $t_k = 0.1 \times 4^k$, $k=3,4,\dots,10$, growing in the direction of the arrow up to $t \approx 1.05 \times 10^5$. The q -Gaussian function with $q=1.53$ was plotted for comparison (solid line). Histograms were shifted for visualization.

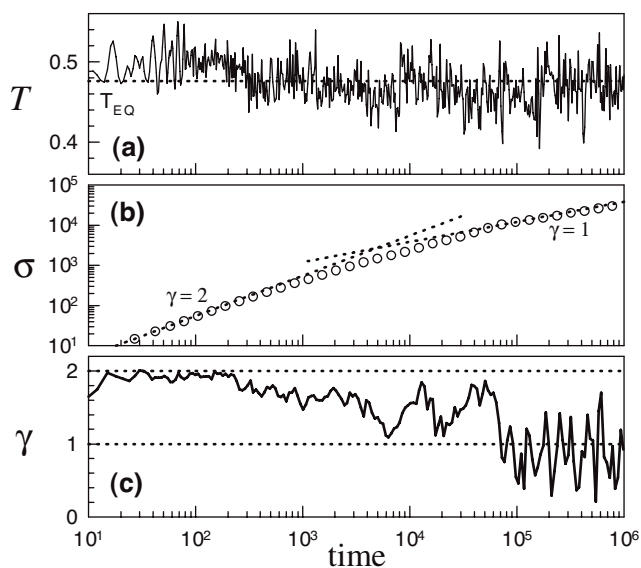


FIG. 5. Time series of (a) temperature T , (b) deviation σ , and (c) diffusion exponent γ , for $N=500$ and $\varepsilon=0.69$. At $t=0$, the system is in an *equilibrium* configuration. The outcome of a single run is exhibited.

For high energies, only the ballistic regime was reported before (in Ref. [11]) since normal diffusion settles at times longer than those analyzed in that work.

For fully magnetized initial conditions, both ballistic and normal regimes are also observed for short and long times, respectively. However, in this case, the crossover is more complex [see Figs. 2(d) and 3(d)]: Exponent γ varies non-monotonically taking superdiffusive values and it does not present a well defined plateau in the same time window as temperature does. For this intermediate stage, superdiffusion has been reported before and attributed to a kind of Lévy-walk mechanism, yielding a succession of free walks and trapping events [11]. Also, it has been interpreted from a topological perspective [17].

The main features that one observes in the profile of local exponent γ versus time [Fig. 2(d)] can be summarized as follows: (i) In a first stage, γ takes a maximum value that remains close to $\gamma=2$, corresponding to ballistic motion. This stage occurs at the beginning of the QS regime and its duration increases with N . (ii) Then γ reaches a minimum value that as N increases falls within the QS range. Also as N increases, the valley broadens and flattens, characterizing a plateau region inside the quasistationary regime. Therefore, for finite sizes, one can detect a superdiffusive phase, in agreement with previous results [11,12]. However, the minimum value of the flat region decays to unity as N increases (see Fig. 3), following an $N^{-1/2}$ law. Thus, anomalous diffusion in QS states is a finite-size effect, an observation already pointed out by Yamaguchi [13] although for a different initial preparation and from a different perspective. (iii) Another maximum appears in correspondence to the rapid relaxation from QS to EQ. The maximal value grows with N , largely exceeding the value $\gamma=2$, but the peak narrows. This peak corresponds approximately to the inflection point in the time evolution of temperature (see Figs. 2 and 3), whose slope

increases with N . In fact, in the QS \rightarrow EQ relaxation, the rapid increase of T (kinetic energy) leads to an accelerated increase of the phases in average. (iv) In the final stage, γ relaxes asymptotically to unity, indicating normal diffusion at very long times.

III. DISCUSSION AND REMARKS

From the analysis of γ , one concludes that diffusive motion in QS trajectories strongly depends on the system size. In the γ versus t profile, as N increases, the neighborhood of the first minimum (inside the QS range defined by T) flattens, defining a quasistationary value of γ . However, this steady value goes to 1 in the TL, as observed in Fig. 3. On the other hand, theoretical calculations from a Klimontovich approach by Bouchet and Dauxois [18] (see also [20]) predict weak anomalous diffusion in the large size limit, implying logarithmic corrections to the normal diffusion law (that would be hardly detectable numerically). However, the Kubo formula employed in those calculations assumes stationarity of the two-time autocorrelation function of velocities, while aging effects have been reported [10]. In any case, our result that diffusion in QS states becomes of the normal type in the TL, in the sense that $\gamma \rightarrow 1$, is in accord with the picture above. This would also be valid for other classes of initial conditions leading to spatially uniform QS states in the continuum limit, as, for instance, water-bag [11], zero magnetization [13], and arbitrary magnetization [21] initial conditions. Moreover, while in the present manuscript the initial preparation is “regular” water-bag, we verified that qualitatively similar results also hold for the usual water-bag preparation.

Furthermore, the spreading of initially confined phases appears to develop long tails. For QS trajectories, histograms adopt a shape that can be described by a q -Gaussian form with q increasing up to a steady value $q \approx 3/2$ (squared Lorentzian). A similar steady value is also attained asymptotically when starting at equilibrium. Probably, the formation of tails is promoted at the initial ballistic stages, which would explain the formation of similar tails both for equilibrium and out-of-equilibrium initial conditions. For both classes of initial conditions, stabilization of parameter q is reached only when γ attains a steady value corresponding to normal diffusion. However, if normal diffusion settles at equilibrium, the squared Lorentzian should not be the final distribution of phases. In agreement with the central limit theorem, the body of the distribution would progressively adopt a Gaussian form. In fact, for instance, a squared Lorentzian evolving through the normal diffusion equation (given by the convolution of the squared Lorentzian with a spreading Gaussian) conserves the power-law tails while becoming Gaussian at the center. However, in such a case the crossover between Gaussian and squared-Lorentzian regimes occurs at times that increase as σ^2 . If a similar process occurs in our case, then the evolution to Gaussianity would only be observable in much longer runs.

Let us note that Lévy densities present power-law tails with exponents restricted to a given interval (yielding divergent second moment) that in terms of parameter q

corresponds to $q > 5/3$, therefore not including the observed values. While the generalization of the standard diffusion equation with fractional spatial derivatives leads to Lévy functions, the nonlinear generalization $\partial_t P(x,t) = D \partial_{xx} [P(x,t)]^{2-q}$, with constant D and q , has q -Gaussian functions as long-time solutions [22]. This nonlinear equation yields anomalous diffusion of the correlated type with exponent $\gamma = 2/(3-q)$. In our case, long tails also develop, however they are characterized by q changing with time and γ is not well-defined. On the other hand, a relation between parameter q arising from a q -exponential fit to momentum

autocorrelations and γ from superdiffusion, namely $\gamma = 2/(3-q)$, has been reported in the literature [23]. The possible connection between these issues and our findings deserves further investigation.

ACKNOWLEDGMENTS

We are grateful to C. Tsallis for fruitful discussions. L.G.M. acknowledges the kind hospitality at Santa Fe Institute, where part of this work was made. We acknowledge Brazilian agency CNPq for partial financial support.

-
- [1] *Dynamics and Thermodynamics of Systems with Long Range Interactions*, Lecture Notes in Physics Vol. 602, edited by T. Dauxois, S. Ruffo, E. Arimondo, and M. Wilkens (Springer, Berlin, 2002), and references therein.
- [2] C. Tsallis, *J. Stat. Phys.* **52**, 479 (1988); *Nonextensive Mechanics and Thermodynamics*, edited by S. Abe and Y. Okamoto, Lecture Notes in Physics Vol. 560 (Springer, Berlin, 2001); in *Non-Extensive Entropy-Interdisciplinary Applications*, edited by M. Gell-Mann and C. Tsallis (Oxford University Press, Oxford, 2004).
- [3] M. Antoni and S. Ruffo, *Phys. Rev. E* **52**, 2361 (1995).
- [4] C. Anteneodo and C. Tsallis, *Phys. Rev. Lett.* **80**, 5313 (1998); F. Tamarit and C. Anteneodo, *ibid.* **84**, 208 (2000); C. Anteneodo and R. O. Vallejos, *Phys. Rev. E* **65**, 016210 (2001); M. C. Firpo and S. Ruffo, *J. Phys. A* **34**, L511 (2001); A. Gian-santi, D. Moroni, and A. Campa, *Chaos, Solitons Fractals* **13**, 407 (2002); B. J. C. Cabral and C. Tsallis, *Phys. Rev. E* **66**, 065101(R) (2002); R. O. Vallejos and C. Anteneodo, *Physica A* **340**, 178 (2004).
- [5] V. Latora, A. Rapisarda, and C. Tsallis, *Phys. Rev. E* **64**, 056134 (2001); *Physica A* **305**, 129 (2002).
- [6] C. Anteneodo and R. O. Vallejos, *Physica A* **344**, 383 (2004).
- [7] Y. Y. Yamaguchi, J. Barré, F. Bouchet, T. Dauxois, and S. Ruffo, *Physica A* **337**, 36 (2004).
- [8] A. Pluchino, V. Latora, and A. Rapisarda, *Physica A* **340**, 187 (2004); *Phys. Rev. E* **69**, 056113 (2004).
- [9] M. A. Montemurro, F. Tamarit, and C. Anteneodo, *Phys. Rev. E* **67**, 031106 (2003).
- [10] A. Pluchino, V. Latora, and A. Rapisarda, *Physica D* **193**, 315 (2004).
- [11] V. Latora, A. Rapisarda, and S. Ruffo, *Phys. Rev. Lett.* **83**, 2104 (1999).
- [12] V. Latora, A. Rapisarda, and S. Ruffo, *Prog. Theor. Phys. Suppl.* **139**, 204 (2000); V. Latora and A. Rapisarda, *Chaos, Solitons Fractals* **13**, 401 (2002).
- [13] Y. Y. Yamaguchi, *Phys. Rev. E* **68**, 066210 (2003).
- [14] D. H. Zanette and M. A. Montemurro, *Phys. Rev. E* **67**, 031105 (2003).
- [15] C. Tsallis, *Physica D* **193**, 3 (2004).
- [16] F. Neri, (unpublished); H. Yoshida, *Phys. Lett. A* **150**, 262 (1990).
- [17] F. A. Tamarit, G. Maglione, D. A. Stariolo, and C. Anteneodo, *Phys. Rev. E* **71**, 036148 (2005).
- [18] F. Bouchet and T. Dauxois, *Phys. Rev. E* **72**, 045103(R) (2005).
- [19] V. Latora, A. Rapisarda, and S. Ruffo, *Physica D* **131**, 38 (1999).
- [20] P.-H. Chavanis, *Physica A* **361**, 81 (2006).
- [21] A. Antoniazzi, D. Fanelli, J. Barré, T. Dauxois, and S. Ruffo, e-print cond-mat/0603813.
- [22] A. R. Plastino and A. Plastino, *Physica A* **222**, 347 (1995); C. Tsallis and D. J. Bukman, *Phys. Rev. E* **54**, R2197 (1996); L. A. Peletier, in *Applications of Nonlinear Analysis in the Physical Sciences* (Pitman, Massachusetts, 1981).
- [23] A. Pluchino, V. Latora, and A. Rapisarda, *Physica A* **338**, 60 (2004).